ISSN: 0852-0682, EISSN: 2460-3945
Forum Geografi, Vol 31 (1) July 2017: 16-27
DOI: 10.23917/forgeo.v31i1.3977

FORUM GEOGRAFI
Indonesian Journal of Spatial and Regional Analysis

Photogrammetry-based Texture Analysis of a Volcaniclastic Outcrop-peel: Low-cost Alternative to TLS and Automation Potentialities using Haar Wavelet and Spatial-Analysis Algorithms

Christopher Gomez[*,1], Kyoko Kataoka[2], Aditya Saputra[3,4], Patrick Wassmer[5], Atsushi Urabe[2], Justin Morgenroth[3], Akira Kato[6,7]
[1] Graduate School of Maritime Sciences, Kobe University, Higashinada-ku, Fukae-Minamimachi 5-1-1, 658-0022 Kobe City, Japan
[2] Niigata University, Research Institute for Natural Hazards & Disaster Recovery. 950-2181 Niigata-City, Nishi-ku, Ikarashi 2nochou 8050, Japan
[3] College of Sciences, Department of Geography, University of Canterbury Christchurch New Zealand
[4] Faculty of Geography, Universitas Muhammadiyah Surakarta
[5] Department of Environment, University of Strasbourg
[6] Paris 1 Sorbonne University LGP Laboratory, Paris, France.
[7] Faculty of Horticulture, Chiba University, Matsudo-city, Chiba-ken, Japan
* Corresponding author (e-mail: christophergomez@bear.kobe-u.ac.jp)

Received: 01 May 2017 / Accepted: 19 June 2017 / Published: 01 July 2017

Abstract. Numerous progress has been made in the field of applied photogrammetry in the last decade, including the usage of close-range photogrammetry as a mean of conservation and record of outcrops. In the present contribution, we use the SfM-MVS method combined with a wavelet decomposition analysis of the surface, in order to relate it to morphological and surface roughness data. The results demonstrated that wavelet decomposition and RMS could provide a rapid insight on the location of coarser materials and individual outliers, while arithmetic surface roughness were more useful to detect units or layers that are similar on the outcrop. The method also emphasizes the fact that the automation of the process does not allows clear distinction between any artefact crack or surface change and that human supervision is still essential despite the original goal of automating the outcrop surface analysis.

Keywords: Structure-from-Motion, Multiple-View Stereophotogrammetry, Wavelet-decomposition, texture analysis, surface roughness, GIS, Spatial Analysis, Close-range Remote Sensing.

Abstrak. *Banyak kemajuan telah dicapai di bidang fotogrametri terapan dalam kurun dekade terakhir, termasuk penggunaan fotogrametri jarak dekat sebagai rujukan konservasi dan perekaman singkapan batuan. Dalam kontribusi sekarang, kami menggunakan metode SfM-MVS yang dikombinasikan dengan analisis dekomposisi wavelet terhadap permukaan lahan, untuk menghubungkannya dengan data morfologi dan kekasaran permukaan. Hasilnya menunjukkan bahwa dekomposisi wavelet dan RMS dapat memberikan wawasan yang cepat mengenai lokasi bahan kasar dan outlier individu, sedangkan aritmatika kekasaran permukaan lebih berguna untuk mendeteksi unit atau lapisan yang serupa pada singkapan batuan. Metode ini juga menekankan fakta bahwa otomatisasi proses tidak memungkinkan perbedaan yang jelas antara retakan artefak atau perubahan permukaan dan bahwa pengawasan manusia masih penting meskipun tujuan awalnya mengotomatisasi analisis permukaan singkapan.*

Kata Kunci: *Structure-from-Motion, stereophotogrammetry multi sudut pandang, dekomposisi wavelet, analisis tekstur, kekasaran permukaan, SIG, analisis spasial, Penginderaan jauh jarak dekat.*

1. Introduction

Science is a product of its time, its imperatives, the technological advances allowing one type of work over another, sometimes the fascination of human for one technology or another. Consequently science can't be fully separated from its social receptacle. As population in countries like Japan are thinning, and that such dwingling always appear after a peak, there is a recurrent pattern of "how do we keep what we used to do, but with less manpower". Such question is meant to come in 40 to 50 years in Indonesia as well.

One way of addressing this issue is to increase automation. In Geology, it means using various tools to employ a machine to do what used to be done by hand. It is within this conceptual framework that the authors have built the present contribution. The aim has therefore been to start developing a method that autmoates some of the outcrop analysis process. In a country, like Indonesia, where population is plenty, this research is also aimed at improving crowd-sourcing automated analysis information.

Outcrops are arguably one of the most important sources of data to study the geology and the geomorphology of volcanic environments. Outcrop analysis is essential – for instance – for calibrating several non-destructive methods, such as ground-penetrating radar (GPR), in volcanic environments where data collection can be challenging (Abrams and Sigurdsson, 2007; Cassidy et al., 2009; Courtland et al., 2012; Finizola et al., 2010; Gomez and Lavigne, 2009; Gomez *et al.*, 2008, 2009, 2012; Gomez-Ortiz *et al.*, 2006; Khan et al., 2007; Lavigne *et al.*, 2007). Despite being a traditional technique, outcrop analysis has recently seen a methodological resurgence with the application of remote sensing (RS) techniques, such as close-range hyperspectral imagery to map mineral content (Buckley et *al.*, 2013) and terrestrial laser scanning, to describe millimeter to centimeter scale features (Bellian *et al.*, 2005). Exploration using these RS techniques has been relatively sparse, most probably because the technical and financial aspects are still prohibitive, and the great majority deals with sub-horizontal surfaces rather than sub-vertical ones (e.g. Heritage and Milan, 2009). Moreover, the contributions – to date – deal mostly with data acquisition and handling rather than obtaining parameters from which one could derive indicators on the nature of the studied material in an automated manner (e.g. Giaccio et al., 2002).

One potential direction that can be explored is the analysis of outcrop surface texture (or surface roughness), which can be a key proxy for environmental processes. This is particularly true in the field of agriculture where surface roughness gives indications on wind deflation, runoff and water absorption, even playing an important part in soil biota and gas exchanges (Vidal Vazquez et al., 2005). Geologists have also used variations of surface texture to characterize different volcanic deposits (Bretar *et al*., 2013) and the mechanisms of rock fragmentation (Tatone and Grasselli, 2009). Surface texture (whether formed by erosion or deposition) also controls electromagnetic scattering on a surface and therefore plays an important role in remote sensing interpretation (Beckmann and Spizzichino, 1987). In this paper, we add to the recent research on using remote-sensing techniques for outcrop analysis. As a key to enter this problem, we explore in the present contribution the question of whether cost-effective remote sensing data acquisition can be used to accurately describe surface texture of volcanic outcrops.

In this paper, we: (1) present Structure–from-Motion associated with Multiple-View Stereophotogrammetry (SfM-MVS), a low-cost alternative to terrestrial laser scanning (Morgenroth and Gomez, 2014) and describe how it could be applied to outcrop-scale analysis; and (2) test various surface texture indicators and the use of wavelet decomposition for surface roughness analysis, in order to determine if these indicators could be used for automatic recognition of granularity and derivation of grain-size variations.

In 1979, Structure-from-Motion (also known as Structure-and-Motion) was first developed in the field of computer-vision engineering (Ullman, 1979). It has since developed into a valuable tool for generating 3D models from 2D imagery (Szelinski, 2011), notably with the development of software with Graphical User Interfaces. Traditional photogrammetry requires a series of identifiable points to be present in at least two photographs and, perhaps more importantly, known values of camera projection, distortion, position, and orientation (Robertson and Cipolla, 2009). By contrast, SfM uses algorithms to identify matching features in a collection of overlapping digital images, and calculates camera location and orientation from the differential positions of multiple matched features (Fisher, *et al.*, 2005; Quan, 2010; Szeliski, 2011). Based on these calculations overlapping imagery can be used to reconstruct a 3D model of the photographed object or scene. Where relative projection geometry and camera position are known the values can be integrated into the SfM reconstruction to improve the calculation productivity and accuracy of the model (Agisoft Photoscan-PRO, 2012).

This study used a commercial software program, Agisoft PhotoScan®-Professional (Agisoft LLC, St. Petersburg, Russia). Although the procedures described in this study are achievable using various free-ware options, the decision to use PhotoScan-Professional software was made because it couples SfM technology with multi-view stereophotogrammetry (MVS) algorithms in a user-friendly interface. Using this combined SfM-MVS approach, the software retrieves an initial set of sparse points from matching features (SfM) and then increases the point-cloud density to improve the reconstruction of the overlying 3D mesh using MVS technology (Agisoft Photoscan-PRO, 2012; James and Robson, 2012; Verhoeven, *et al*., 2012).

In order to numerically study the variations of a surface from an ideal general shape, a series of tools are available, spanning from descriptive statistical indicators to more complex fractal-based (Bretard, *et al*., 2013) and wavelet-based analysis (Gomez, 2012) allowing measures at various scales (Gomez, 2013).During the last 10 years, the use of wavelet analysis in earth-sciences has increased concomitantly with the increasing availability of numerical data. It has especially benefited from the study of time-series for the determination of different frequencies and momentums (e.g. Andreo *et al.*, 2006; Partal and Küçük 2006; Rossi *et al.,* 2009). Analyses of space-scale data with wavelet - although more scarce in earth-sciences – are also on the rise (e.g. Audet and Mareschal, 2007; Booth *et al.*, 2009; Lashermes *et al.,* 2007), eventually following the influence of research in medical imagery, which has been widely using wavelet for topographical analysis for instance (e.g. Langenbucher *et al.*, 2002).

Wavelets allow the decomposition of a signal into a set of approximations, which is hierarchically organized in a combination of different scales. Wavelet analyses use a short-term duration wave as a kernel function in an integral transform. There are several types of wavelet, which are named after their inventors: e.g. Morlet wavelet, Meyer wavelet. Based on the shape of the series/function that needs to be analyzed, the appropriate mother wavelet is scaled and translated (daughter wavelet), allowing the detection of the different frequencies of a signal at different time (Torrence and Compo 1998; Schneider and Farge, 2006). This mathematical transform can be very useful to study surface variations of large-scale topography or localized surface texture Wavelet is a well-fitted tool for separating spectral components of topography (i.e. working on different scales of a single object), because it gives both the spatial and the spectral resolution. Consequently, it is a mathematical tool that reproduces some of the abstraction that human being do when looking at an outcrop or any other object, separating the different scales to make sense of the objects they are linked to.

2. Research Method

a. Location

Japan is a volcanic archipelago that seats on the Pacific Ring of Fire and it is arguably one of the most tectonically and volcanically active regions in the world. Numazawa Volcano is located on the main island of Japan, Honshu (Figure 1), in the western part of Fukushima Prefecture and about 50 km west of the volcanic front (Yamamoto, 2007; Kataoka et al., 2008). Numazawa Volcano (835 m a.s.l. at the peak Maeyama) has developed on the edge of the Uwaigusa caldera complex (Yamamoto and Komazawa, 2004). The volcano encompasses a caldera lake in 2 km diameter and ~100 m deep at the level about 475 m a.s.l. Chronologically, the volcaniclastic deposits generated by Numazawa volcano are: the 110 k.a. Shibahara pyroclastic deposits; the 71 k.a Mukuresawa lava dome; the ~50 k.a Mizunuma pyroclastic-flow deposits; the Sozan lava dome of 43 k.a; the Maeyama lava dome of 20 k.a and the Numazawako eruption of 5.4 k.a (Yamamoto, 2007). Kataoka et al. (2008) have described in details an outburst flood from a temporal dam lake formed in the Tadami River valley by the Numazawako ignimbrite emplacing eruption and its geomorphic impacts around the volcano, including the flood terraces in the Tadami River, from which the material used in the present contribution has been extracted (Cf. Figure 9 in Kataoka et al., 2008). The 290 cm high x 85 cm wide outcrop-peel was extracted from the flood deposits with multiple inversely graded bed sets, rich in rounded pumices indicative of a hyperconcentrated flow deposition (Kataoka et al, 2008). The deposit is dominated by coarse sand to pebble size material. The peel is part of a 15 m thick unit that lied on top of debris-flow deposits.

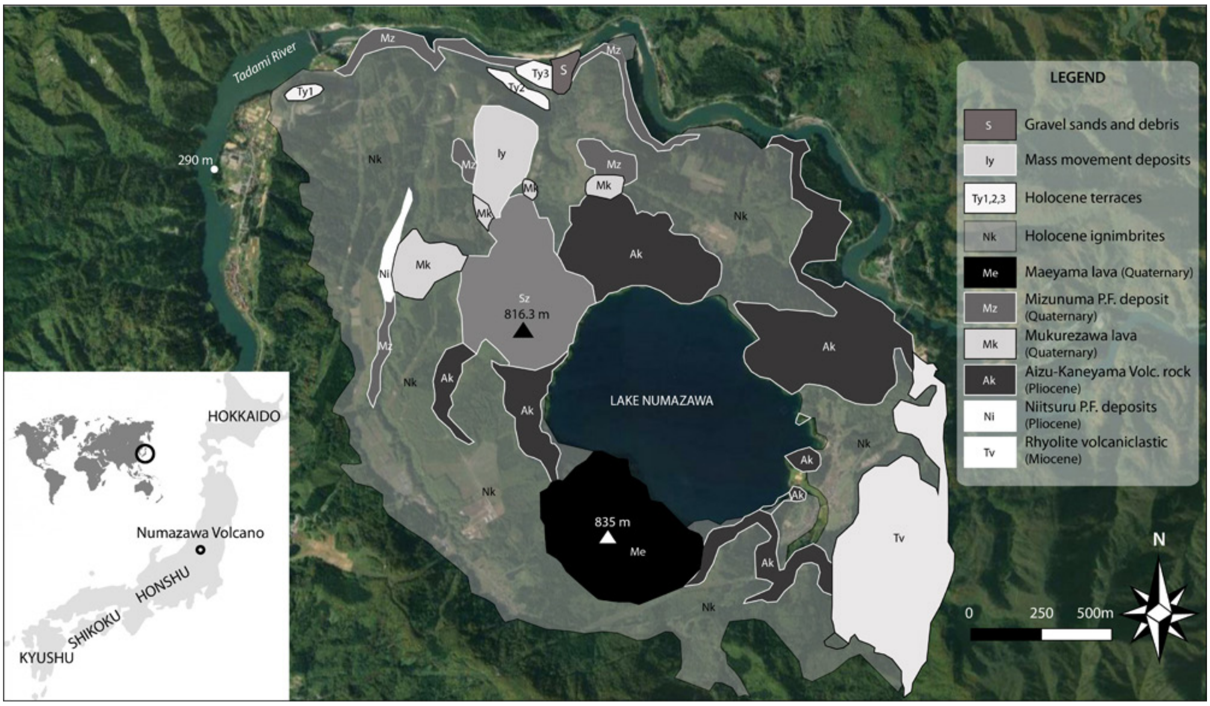

Figure 1. Location of Numazawa Volcano in Japan and distributon of the major volcanic units on the volcano. source: Yamamoto and Komazawa, 2004; drawn from: Geological Survey of Japan - https://gbank.gsj.jp/volcano/Act_Vol/numazawa/page3.html)

b. Data Collection and Analysis

For the present study, a sandy to gravely material from Numazawa Volcano (Japan) has been digitally acquired and analyzed. The digital data has been collected using a point and shoot digital camera (Canon cybershot), by 'hovering' over the outcrop taking 170 photographs from a distance of 10 to 40 cm. The method for image acquisition may differ depending on the algorithm used (e.g. Figure 1 in Westoby, 2012). In this study, photographs were taken to maximize the overlap such that features of the outcrop were captured by multiple photographs.

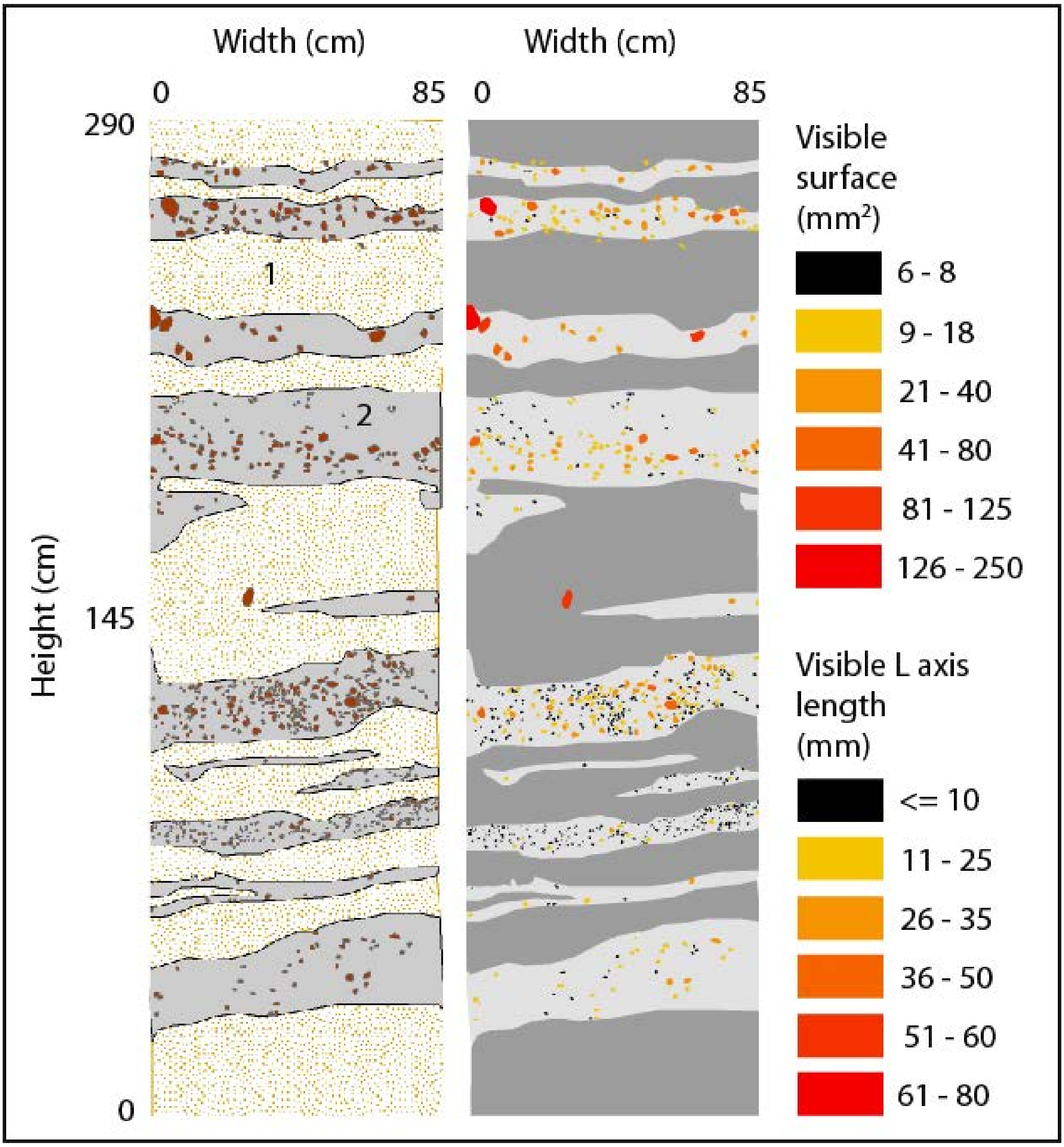

Figure 2. Outcrop reconstruction from the SfM-MVS derived collated orthorectified and scaled referenced imagery. The outcrop representation on the left displays the main sedimentary structures with mix-sand and coarse sand matrix (1) layers; and coarse-sand to small pebbles matrix layers (2). Larger Pebbles – mostly pumices – of significant size were individually recorded and measured with the visible L-axis (long-axis) and the visible area, as displayed on the right representation of the outcrop.

Using PhotoScan–professional, we applied the SfM technique to reconstruct a point-cloud based solely on the uncalibrated photographs, with tie-points of known location (x,y,z) in order to constrain the point-cloud in 3D. We subsequently used the MVS technique to build a 3D surface from the 3D point-cloud and camera location calculated by SfM. The 3D mesh was exported as both a vector model and a pixel based map.

Data were then exported into (1) the GIS environment ArcGIS® (ESRI, Redlands, CA, USA)and (2) the MATLAB® (MathWorks, Inc, Natick, MA, USA) programming environment. In the GIS environment, the 3D surface created from SfM-MVS was loaded as a single layer and transformed into a tiff file that can be recognized as a 3 level matrix in Matlab. The dataset was then transferred into the Matlab programming environment to conduct the examination and measures of surface texture-variations/roughness using a series of different mathematical tools: (a) wavelet decomposition; (b) arithmetic average roughness; and (c) proximity analysis of positive and maximum negative variation in a square of 2x2 cm. The algorithms were implemented using 'cellular automata-type' series of scripts. The acquisition and processing methods have been then discussed to present the limits and potentials of the different method.

3. Results

a. Visual description from 3D digital outcrop

Using the visual results of the SfM-MVS recomposition, a series of beds of medium to coarse sands and pumice pebbles have been identified in the 2.9 m interval (Figure 2). These pumice clasts have a main axis (L) of the range ~10 to 80 mm (as measured from the 3D digital outcrop) and a visible surface of 8 to 250 mm^2 (Figure 2). Most individual layers dominated by sand grains and centimetres to decimeters thick contain pimice pebble and cobble unevenly distributed except for an isolated single large pumice located at 145 cm height. In the upper half of the outcrop, mostly pumice clasts display characteristics of L>51 mm located between 145 cm and 290 cm height, and only 3 clasts of 36 mm < L < 50 mm are located in the bottom half of the outcrop. The SfM-MVS visual reconstruction can therefore yield useful information in terms of distributions (part of grainsize) and axes orientations of clasts for a traditional outcrop visual analysis (Cf. visual in Figure 3-a), but more importantly SfM-MVS also reconstructed the surface 'vertical topography' of the outcrop (Figure 3).

b. Haar-wavelet decomposition as a tool to study micro-variations

The vertical topography of the outcrop peel derived from SfM-MVS has been tied on a perfectly vertical wall, and therefore a slight slant of 6 cm over the 290 cm height of the outcrop-peel appears. In order to perform localized analysis of the surface variations, the general slope of the surface has been subtracted using wavelet decomposition (Figure 3-c,d,e). The resulting variation is shown in Figure 3-e, where only the variations independent from the general sloping trend have been conserved. This transformation has put the emphasis of the lower part of the outcrop where numerous micro-topography variations were disappearing in the general slope acceleration (see the discussion for the interpretation of this slope). In the upper part of the outcrop, just above and below the 500 sampling point, one can observe - in Figure 3-e – the strong variation of the signal and link them to two units of coarser material including larger clasts of centimeter-scale (Figure 3-a & Figure 2).

Since the different levels of wavelet decomposition are scale-related, we have used the lowest level of the Haar-wavelet decomposition (Figure 4) in order to detect the finer micro-variations of the outcrop along 7 vertical transects equally spaced between 10 cm and 70 cm. This analysis has yielded positive results with variations in the coarser units being clearly detected in 'A', 'B' and 'F' (Figure 4). Local inclusions of larger size pumice clasts have also influenced the signal (Figure 4-C). In the same manner, sandy layers without inclusion of large clasts or pebbles have displayed smoother signal traces with limited amplitude (Figure 4-D). The signal also reacted to microvariations that are not due to grain-size variations, but linked to the fracture of the outcrop-peel itself. One can also observe the desiccation holes and cracks (Fig 4-E) and those created by peeling and transportation of the outcrop-peel (Figure 4-G). The effects of the micro-rills located at the bottom of the outcrop – and which did not appear strongly in the combined levels of the wavelet decomposition (Figure 3-E) – have created strong amplitude variations in the lowest level of the wavelet decomposition (Figure 4-H).

Wavelet decomposition has shown to be a useful tool to automate processes such as detrending and surface roughness patterns, but the reasons behind the signal micro-variations can have various sources limiting an automated recognition system based solely on wavelet decomposition.

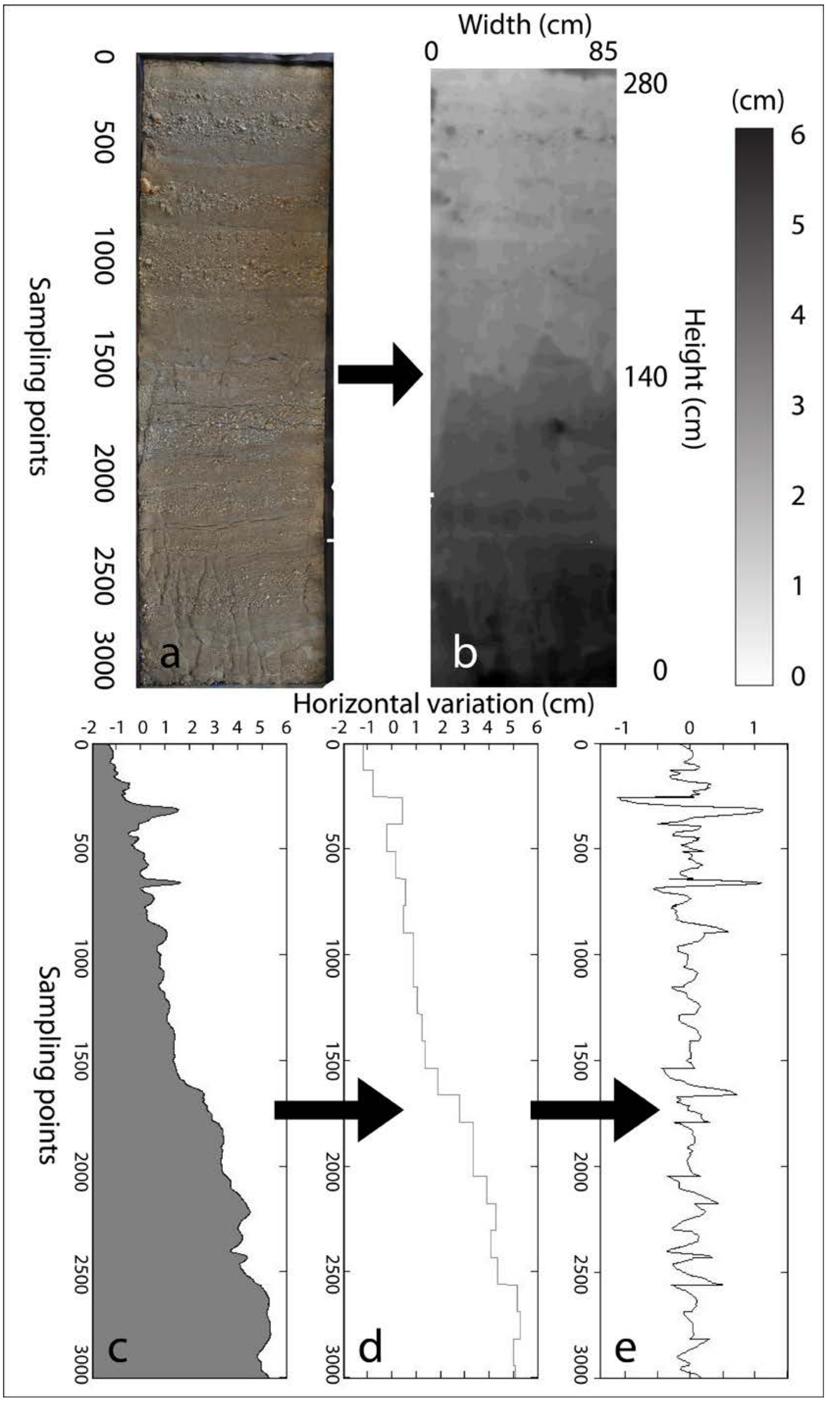

Figure 3. Detrending using wavelet. Transformation of the surface 'topography' obtained from Structure From Motion. (a) Orthophotograph constructed from Structure from Motion; (b) Surface variation, the 0 being the perfect vertical; (c) Surface extraction of the vertical transect at the centre of the outcrop; (d) 'topographic' general trend as extracted by Haar wavelet decomposition (Level 7 of a 7 scales decomposition); (e) Combination of the 4 lowest level of wavelet decomposition minus the main trend at level 7 (e = L1+L2+L3+L4-L7). One will note that (b) is only coded to 280 cm height as the upper part also includes the wood frame around the peel, which creates strong micro-topographic variations spreading the variation scale and thus limiting the graphic quality of the output.

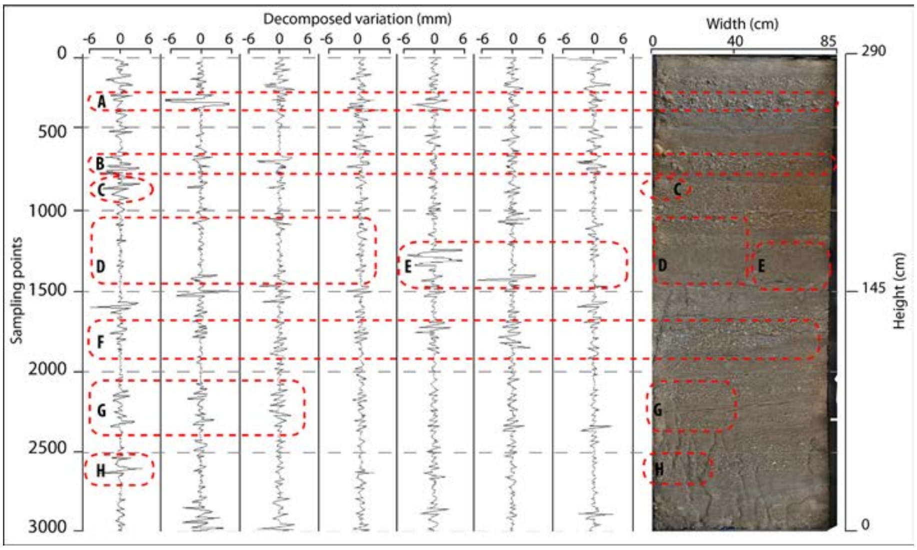

Figure 4. Wavelet decomposition of the outcrop at level 1 (out of a 7 levels decomposition using a Haar mother-wavelet). As the lowest level reacts to the shortest variations in space, this analysis was performed to detect the microvariations (this lowest level is often considered as the 'white-noise' in signal processing).

c. Statistical and Spatial Analysis to detect surface roughness micro-variations

The indicators used in the present section are normally used to detect microvariations in GIS and in the manufacturing industry. Although the instrumentation and the scale are different the underlying algorithms are similar. The first indicator tested is the arithmetic roughness average (R_a), which gives indications of the localized maximum variation (Figure 5). This algorithm, computed over an average moving window of 2 cm^2 has been successful at identifying rapid localized variations generated by increased roughness due to the coarseness of the matrix (Figure 5-b,d). It also succeeded at identifying smoother material on the outcrop (Figure 5-a,c,e) and defining their smaller scale variations. Indeed the variation of coarse material is in the order of x*10^{-3} m, while finer material varies in the order of x*10^{-4} m from local average variation (one will note that these later variations are below the mm scale and most certainly fall within the error of margin of data acquisition).

The second algorithm tested with a relative success is the RMS:

$$[(\frac{1}{L}\int_0^L Z(x)^2 dx]^{1/2} \quad \text{.........................} \quad (1)$$

It calculates the root mean square of the squared variation values from an ideal surface – in the present case the detrended surface.

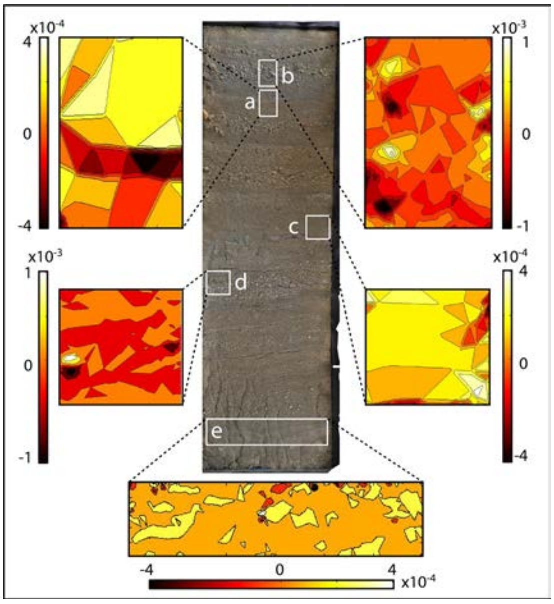

Figure 5. Arithmetic average roughness (R_a) extracted using a 2cm x 2cm moving average detrending, which reduces the effects of large variation on the outcrop. (a & c) R_a of coarse sand units; (b & d) R_a of coarser sand with gravels and centimetric clasts inclusions; (e) R_a of coarse sand with several vertical erosional rill remnants. It is interesting to note that R_a did not react to these variations (one will note that the scales of a,c and e are the same but b and d differ in order to display the variations at different scales).

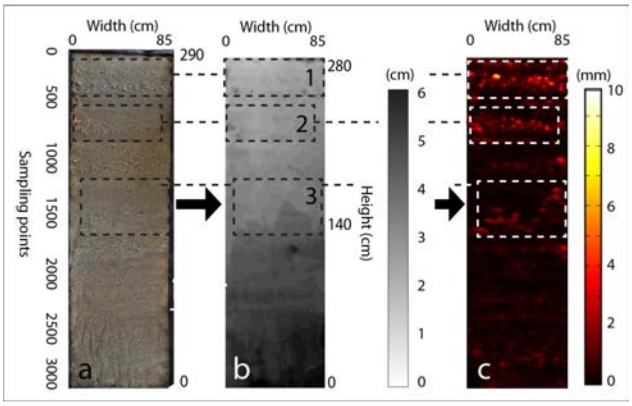

Figure 6. RMS or square root of the square of local variation from the entire detrended surface. This index allows finding elements that protrude locally from the surrounding, such as isolated gravels in finer material, etc. The profile (a) is the reconstructed photograph using textured SfM-MVS; the profile (b) is the surface microtopography from an idea vertical; profile (c) is the dvar. On the three profiles box 1,2 and 3 have been drawn for regions of interests (see the text for full comments on these boxes).

The result of the RMS shows the ability of the algorithm to detect and individualize local variations, such as the presence of the centimeter-scale clast inclusions (Figure 6-1&2), but it also detects quick variations such as the edge of a layer slightly protruding from the rest of the outcrop (Figure 6-3).

4. Discussion and Concluding Remarks

The different algorithms using wavelet and spatial statistics techniques tested here on the SfM-MVS derived data have shown their ability to produce measures of the surface roughness. It also shows that the SfM-MVS is a method that can successfully capture microtopographic variations on outcrops even at the millimeter level. The intrinsic advantage of this workflow is its low-cost (e.g. of topographic application: Westoby et al., 2012) and the fact that anybody can go and collect data for the scientist to process, as it only requires standard overlapping photographs from a low-cost, off-the-shelf camera. However, the surface roughness processing algorithms tested here are not sufficiently developed to automate the process of recognizing layers of coarser grain-size or the presence of larger clasts in a series as they also reacts to the imperfections of the outcrop.

Although the detection of these imperfections hamper the full-automation of the process in the present study, the behavior of these algorithms could be used to detect the imperfections on rock-faces, which Giaccio et al. (2002) measured using a roughness-meter, and used as a proxy of erosion features invisible to the naked eye . Although the 'manual processing and interpretation' of data captured with a roughness-meter or even non-contact methods such as SfM-MVS or TLS is possible, it is necessary to improve the speed of data processing for large-surface outcrop, outcrop peels or event potential use on rock faces.

Despite portability, low-cost and low-logistic demand, SfM-MVS is extremely time-consuming during the processing process (Westoby et al., 2012). Using a four core E7 at 2GhZ CPU and 6GB RAM the SfM-MVS process reached almost 30 hours computing. It has been suggested that this lengthy process could be reduced by diminishing the resolution of the photographs, though this may result in loss of detail, then in the density of keypoints and thus, the final quality of the reconstructed surface may be diminished. Such suggestion works for work at the landscape scale, but for our study we were interested by micro-variations and therefore working at a sub-centimeter to centimeter level, it is therefore important to keep the full-resolution of the photographs, in which case the speed of processing can only be accelerated using more powerful computers.

The development of this method, the need for powerful algorithms and the hardware limitation are symptomatic of the recent shift in the geo-sciences technical paradigms, where data is widely available and easy to collect (compared to ~30 years ago) and is now less of a challenge than the processing of data too numerous to be effectively processed in a timely manner. Such a shift and necessity is also perceptible in the funding strategies like the late y.2013 NSF grant 'EarthCube', aiming to develop cyber-infrastructure in earth-sciences.

One also has to be careful of the significance of the data that are collected. Indeed, although the present sediment peel is used as a support to present a wavelet-based analysis of SfM-MVS collected data, the results are only significant for a very small portion of an outcrop and they are also constrained by the technique that was used to create the outcrop. Indeed some of the topgoraphic features extracted from the peel sample can be linked to the technique. It is indeed most probable that some of the outcrop features are due to the outcrop surface that had a slope and that allowed the glue to penetrate some layers more than others, so that more sediments "clinged" to the peel.

Finally, SfM-MVS is a rapid method to collect very fine outcrop data in the field, and could be extensively used on volcanoes, because it would allow the preservation of orthorectified and georeferenced outcrop morphologies and images, which would be extremely useful for comparisons after volcanic evolutions, especially on volcanoes that change extremely quickly. Such extended dataset are therefore in need of algorithms providing partial or full-automation of some of the processing steps. It appears that wavelet decomposition and RMS would provide a rapid insight on the location of coarser materials and individual outliers, while arithmetic surface roughness would be more useful to detect units or layers that are similar on an outcrop.

5. References

Abrams, J. Sigurdsson, H. (2007) Characterization of pyroclastic fall and flow deposits from the 1815 eruption of Tambora volcano, Indonesia using ground-penetrating radar. *Journal of Volcanology and Geothermal Research. Vol. 161, pp. 352-361.*

Andreo, B. Jimenez, P. Duran, J.J. Carrasco, F. Vadillo, I. Mangin, A. (2006) Climatic and hydrological variations during the last 117-166 years in the south of the Iberian Peninsula, from spectral and correlation analysis and continuous wavelet analysis. *Journal of Hydrology. Vol. 324, pp. 24-39.*

Agisoft Photoscan-PRO Users Manual, (2012) http://downloads.agisoft.ru/pdf/photoscan-pro_0_9_0_en.pdf - accessed in November 2012.

Audet, P. Mareschal, J-C. (2007) Wavelet analysis of the coherence between Bouguer gravity and topography: application to the elastic thickness anisotropy in the Canadian Shield. *Geophysics Journal International. Vol. 168, pp. 287-298.*

Beckmann, P. Spizzichino, A. (1987) *The scattering of electromagnetic waves from rough surfaces*. Artech House.

Bellian, J.A. Kerans, C. Jennette, D.C. (2005) Digital outcrop models: applications of terrestrial scanning lidar technology in stratigraphic modeling. *Journal of Sedimentary Research. Vol. 75, pp. 166-176.*

Booth. A.M. Roering, J.J. Taylor Perron, J. (2009) Automated landslide mapping using spectral analysis and high-resolution topographic data: Puget Sound lowlands, Washington, and Portland Hills, Oregon. *Geomorphology. Vol. 109, pp. 132-147.*

Bretar, F. Arab-Sedze, M. Champion, J. Pierrot-Deseilligny, M. Heggy, E. Jacquemoud, S. (2013) An advanced photogrammetric method to measure surface roughness: Application to volcanic terrains in the Piton de la Fournaise, Reunion Island. *Remote Sensing of Environment. Vol. 35, pp. 1-11.*

Cassidy, N.J. Calder, E.S. Pavez, A. Wooler, L. (2009) GPR-derived facies architectures: A new perspective on mapping pyroclastic flow deposits. *Special Publication of IAVCEI. Vol. 2, pp. 181-210.*

Courtland, L.M. Kruse, S.E. Connor, C.B. Savov, I.P. Martin, K.P. (2012) GPR investigation of tephra fallout, Cerro Negro volcano, Nicaragua: A method for constraining parameters used in tephra sedimentation models. *Bulletin of Volcanology. Vol. 74, pp. 1409-1424.*

Buckley, S.J. Kurz, T.H. Howell, J.A. Schneider, D. (2013) Terrestrial lidar and hyperspectral data fusion products for geological outcrop analysis. *Computers and Geosciences. Vol. 54, pp. 249-258.*

Finizola, A. Ricci, T. Delana, R. Cabusson, S.B. Rossi, M. Praticelli, N. Giocoli, A. Romano, G. Delcher, E. Suski, B. Revil, A. Menny, P. Di Gangi, F. Letort, J. Peltier, A. Villasante-Marcos, V. Douillet, G. Avard, G. Lelli, M. (2010) Adventive hydrothermal circulation on Stromboli volcano (Aeolian Islands, Italy) revealed by geophysical and geochemical approaches: implications for general fluid flow models on volcanoes. *Journal of Volcanology and Geothermal Research. Vol. 196, pp. 111-119.*

Fisher, R.B., Dawson-Howe, K., Fitzgibbon, A., Robertson, C., Trucco, E., 2005. *Dictionary of Computer Vision and Image Processing*. Wiley, Chichester.

Giaccio, B. Galadini, F. Sposato, A. Messina, P. Moro, M. Zreda, M. Cittadini, A. Salvi, S. Todero, A. (2002) Image processing and roughness analysis of exposed bedrock fault planes as a tool for paleoseismological analyisis: results from the Campo Felice fault (central Apennines, Italy). *Geomorphology. Vol. 49, pp. 281-301.*

Gomez C. (2013) Scales in Environmental Sciences, Public Lecture, University of Chiba 8 Jan. 2013.

Gomez, C. (2012) Multi-scale topographic analysis of Merbabu and Merapi volcanoes using wavelet decomposition. *Environmental Earth-Sciences. Vol. 65, pp. 1423-1430.*

Gomez, C. Kataoka, K.S. Tanaka, K. (2012) Internal structure of the Sanbongi Fan-Towada Volcano, Japan: Putting the theory to the test, using GPR on volcaniclastic deposits. *Journal of Volcanology and Geothermal Research. Vol. 229-230, pp. 44-49.*

Gomez, C. Lavigne, F. (2010) Transversal architecture of lahars terraces, inferred from radargrams: preliminary results from Semeru Volcano, Indonesia. *Earth Surface Processes and Landforms. Vol. 35, pp. 1116-1121.*

Gomez, C. Lavigne, F. Hadmoko, D.S. Lespinasse, N. Wassmer, P. (2009) Block-and-ash flow deposition: A conceptual model from a GPR survey on pyroclastic-flow deposits at Merapi Volcano, Indonesia. *Geomorphology. Vol. 110, pp. 118-127.*

Gomez, C. Lavigne, F. Lespinasse, N. Hadmoko, D.S. Wassmer, P. (2008) Longitudinal structure of pyroclastic-flow deposits, revealed by GPR survey at Merapi Volcano, Java, Indonesia. *Journal of Volcanology and Geothermal Research. Vol. 176, pp. 439-447.*

Gomez-Ortiz, D. Martin-Velazquez, S. Martin-Crespo, T. Marquez, A. Lillo, J. Lopez, I. Carreno, F. (2006) Characterization of volcanic material using ground penetrating radar: A case study at Teide Volcano (Canary Islands, Spain). *Journal of Applied Geophysics. Vol. 59, pp. 63-79.*

Heritage, G.L. Milan, D.J. (2009) Terrestrial Laser Scanning of grain roughness in a gravel-bed river. *Geomorphology. Vol. 113, pp. 4-11.*

James, M.R. Robson, S. (2012) Straightforward reconstruction of 3D surfaces and topography with a camera: Accuracy and geoscience application. *Journal of Geophysical Research. Vol. 117, F03017, doi:10.1029/2011JF002289,2012.*

Kataoka, K.S. Urabe, A. Manville, V. Kajiyama, A. (2008) Breakout flood from an ignimbrite-dammed valley after the 5 ka Numazawako eruption, northeast Japan. *Geological Society of America Bulletin, Vol. 120, pp. 1233-1247.*

Khan, S.D. Heggy, E. Fernandez, J. (2007) Mapping exposed and buried lava flows using synthetic aperture and ground-penetrating radar in Craters of the Moon lava field. *Geophysics. Vol. 76, B161-B174.*

Langenbucher, A. Sauer, T. Seitz, B. (2002) Wavelet analysis of corneal topographic surface characterization. *Current Eyes Research, Vol. 24, pp. 409-421*

Lashermes, B., Foufoula-Georgiou, E., Dietrich, W.E. (2007) Channel network extraction from high resolution topography using wavelets. Geophysical Research Letters 34, L23S04

Lavigne, F., Thouret, J.-C., Hadmoko, D.S., Sukatja, B. (2007) Lahars in Java: Initiations, Dynamics, Hazard Assessment And Deposition Processes. *Forum Geografi* 21.

Morgenroth, J. Gomez, C. (2014) Assessment of tree structure using a 3D image analysis technique – a proof of concept. *Urban Forestry and Urban Greening. Vol. 13, pp. 198-203.*

Partal, T. Küçük, M. (2009) Long-term trend analysis using discrete wavelet components of annual precipitations measurements in Marmara region (Turkey). *Physics and Chemistry of the Earth. Vol. 31, pp. 1189-1200*

Quan, L. (2010) *Image-based Modeling*. Springer, New York.

Robertson, D.P. Cipolla, R. (2009) Structure from motion. In: Varga, M. (Ed.), *Practical Image Processing and Computer Vision*. John Wiley and Sons, Ltd, New York.

Rossi, A. Massei, N. Laignel, B. Sebag, D. Copard, Y. (2009) The response of the Mississippi River to climate fluctuations and reservoir construction as indicated by wavelet analysis of streamflow and suspended-sediment load, 1950-1975. *Journal of Hydrology. Vol. 377, pp. 237-244.*

Schneider, K. Farge, M. (2006) Wavelets: theory. In: Françoise JP, Naber G, Tsun TS (Eds.), *Encyclopedia of Mathematics Physics, pp. 426-438*

Szeliski, R. (2011) *Computer Vision. Algorithms and Applications*. Springer, New York.

Tatone, B.S.A. Grasselli, G. (2009) A method to evaluate the three-dimensional roughness of fracture surfaces in brittle geomaterials. The Review of Scientific Instruments. *Vol. 80, nb. 125110.*

Torrence, C. Compo, GP. (1998) A practical guide to wavelet anlysis. *Bulletin of the American Meteorological Society. Vol. 79, pp. 61-78.*

Verhoeven, G. Doneus, M. Briese, Ch. Vermeulen, F. (2012) Mapping by matching: a computer vision-based approach to fast and accurate georeferencing of archaeological aerial photographs. *Journal of Archaeological Science, Vol. 39, pp. 2060-2070.*

Vidal Vazquez, E. Vivas Miranda, J.G. Paz Gonzalez, A. (2005) Characterizing anisotropy and heterogeneity of soil surface microtopography using fractal models. *Ecological Modelling. Vol. 182, pp. 337-353.*

Ullman, S. (1979) The interpretation of structure from motion. *Proceedings of the Royal Society of London. Vol. B-203, pp. 405-426.*

Westoby, M.J. Brasington, J. Glasser, N.F. Hambrey, M.J. Reynolds, J.M. (2012) 'Structure-from-Motion' photogrammetry: A low-cost, effective tool for geoscience applications. *Geomorphology, Vol. 179, pp. 300-314.*

Yamamoto, T. (2007) A Rhyolite to dacite sequence of volcanism directly from the heated lower crust: Late Pleistocene to Holocene Numazawa volcano, NE Japan. *Journal of Volcanology and Geothermal Research, Vol. 167, pp. 119-133.*

Yamamoto, T., Komazawa, M. (2004) Geology of the Miyashita District Quadrangle Series, 1:50,000, Geological Survey of Japan, AIST, 71 p.